



## IDENTIFICATION OF NONLINEAR SITE RESPONSES OF VERTICAL MOTIONS BASED ON VELOCITY WAVEFORMS

T. Satoh<sup>(1)</sup>

<sup>(1)</sup> Research Fellow, Shimizu Corporation, [toshimi.satoh@shimz.co.jp](mailto:toshimi.satoh@shimz.co.jp)

### Abstract

Nonlinear site responses of horizontal motions are well known and have been studied by many researchers. However, nonlinear site responses of vertical motions have not been payed attention to so much in the field of strong motion studies. On the other hand, it was pointed out that vertical motions were generated due to the dilatancy or volume change of soil by experimental or analytical studies on elasto-plastic dynamic of soil (e.g. Oshima and Watanabe. 1994). Morio et al. (2017) showed that both horizontal and vertical ground motions at K-NET Tsukidate during the 2011 Tohoku earthquake with JMA seismic intensity scale of 7 were affected by negative dilatancy, that it, contraction by analytical studies. We show that the existence of nonlinear site responses of vertical motions is identified by velocity waveforms integrated from acceleration records observed at the ground surface using KiK-net records. In the case of the generation of nonlinear site responses of vertical motions, the velocity waveform has a linear trend to the downward direction and then becomes constant or almost constant. In some cases, the velocity time history abruptly becomes constant like as a step function. We define the absolute constant value as  $V_{non}$ . The surface-to-borehole spectral ratios of vertical strong motions with such features have the peaks at the same or double of the peak frequencies of the horizontal strong motions. The features that the predominant frequencies of vertical motions are double of those of horizontal motions suggest dilatancy effects as pointed out by the previous studies. The spectral ratios of vertical strong motions tend to be larger than those of weak motions in the frequency less than about 10 Hz. The peak amplitudes of spectral ratios of horizontal strong motions at half of peak frequencies of vertical strong motions also tend to be larger than those of weak motions. The strong motions with three biggest  $V_{non}$  were records observed at KiK-net Haga during the 2011 Tohoku earthquake, KiK-net Oiwake during the 2018 Hokkaido Iburi-Tobu earthquake and KiK-net Hino during the 2000 Tottori-ken Seibu earthquake. The acceleration waveforms and the particle orbits show the features suggesting the dilatancy shown analytically by Morio et al. (2017). These strong motions were equivalent to JMA instrumental seismic intensity scale of 7. The  $V_{non}$  of K-NET Tsukidate was the biggest among all KiK-net records. Since the dilatancy influenced on both horizontal and vertical site responses, these large ground motions might be affected by nonlinear site responses with the dilatancy. The other plausible interpretation of  $V_{non}$  is the settlement of the ground due to the dissipation of the excess pore water pressure, since some acceleration records have spiky-shape suggesting the increase of the excess pore water pressure.

**Keywords:** Nonlinear site response; Vertical ground motion; Dilatancy; Velocity waveform; KiK-net record



## 1. Introduction

Nonlinear site responses of horizontal motions are well known and have been studied by many researchers. However, nonlinear site responses of vertical motions have not been payed attention to so much in the field of strong motion studies. On the other hand, it has been pointed out that vertical motions are generated due to the dilatancy or volume change of soil by experimental or analytical studies on elasto-plastic dynamic of soil (e.g. [1, 2]). Morio et al. [2] showed that both horizontal and vertical ground motions at K-NET Tsukidate (MYG004) during the 2011 Mw9.0 Tohoku earthquake with JMA seismic intensity scale of 7 were affected by negative dilatancy, that it, contraction of soil by analytical studies. It has pointed out [1, 2] that vertical motions are dominant at double frequencies of horizontal motions due to dilatancy.

In this study we show that the existence of nonlinear site responses of vertical motions is identified by velocity waveforms integrated from acceleration records observed at the ground surface. We also show that the peak frequencies of surface-to-borehole spectral ratios of vertical motions are double of those of horizontal motions in the case of the existence of the nonlinear site responses for vertical motions. This study was written in [3] in Japanese.

## 2. Data and Method

We select strong motions with peak ground accelerations (PGAs) of vector of three components of KiK-net acceleration records [4] from 1997 to 2018. After the zero-line correction using the average of pre-event memory, velocity time histories are calculated by integration of the acceleration records in the time domain. Fig.1 shows acceleration records and the integrated velocity time histories at the ground surface of KiK-net Oiwake (IBUH01) during the 2018 Mw6.6 Hokkaido Iburi-Tobu earthquake. The strong motions were equivalent to JMA seismic intensity scale of 7 [4]. The velocity waveform of horizontal component has a liner trend. This is a usual feature of large ground motions of horizontal and vertical components of KiK-net and K-NET records (e.g. [5, 6]). However, the velocity waveform of vertical component has a linear trend to the downward direction and then becomes constant. This feature is observed only in some vertical components with large amplitudes but not observed in any horizontal components. We define the absolute of the constant velocity value as Vnon. Red lines in Fig.1 are models fitting to the velocity waveforms. Fig.2 illustrates four types models of velocity waveforms of vertical components with Vnon. The waveform at IBUH01 is modeled by Model-i0. Most of waveforms are modeled by Model-i0. In some cases, waveforms are modeled by Model-s0, Model-i+ and Model-i-. In Mode-s0, Vnon is generated like the step function.

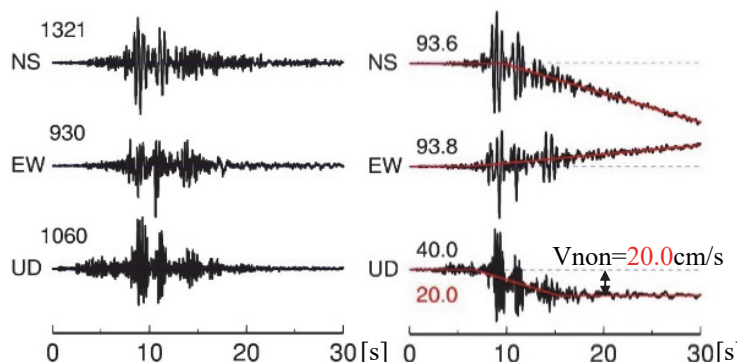


Fig. 1 – Acceleration records (left) and the integrate velocity records (right) observed at the ground surface of KiK-net Oiwake (IBUH01) during the 2018 Hokkaido Iburi-Tobu earthquake. Vnon is defined as the absolute of constant velocity value [cm/s]. Red lines indicate the models of velocity waveforms. Black numbers indicate peak ground accelerations [cm/s<sup>2</sup>] and velocities [cm/s] in 30 s.

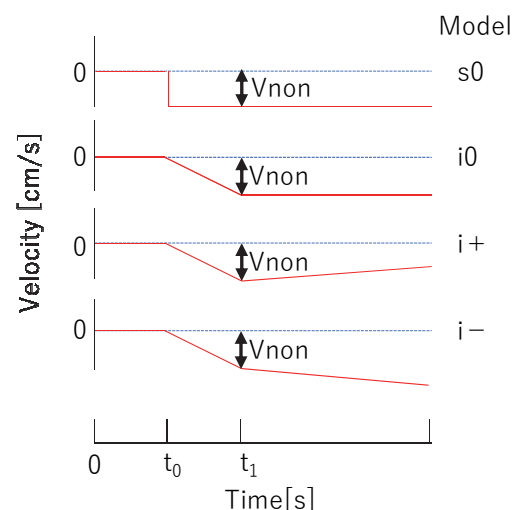


Fig. 2 – Models of velocity waveforms of vertical components with Vnon



Total 48 data among 302 strong motions of vertical components have Von. Fig.3 shows the PGAs of horizontal and vertical components without and with Vnon. PGAs of strong motions with Vnon are larger than those without Vnon in general except strong motions observed at KiK-net IWTH25 (Ishinoseki-Nishi) during the 2008 Mw6.8 Iwate-Miyagi Nairiku earthquake (20080614). Fig.4 shows the locations of the epicenters (JMA) with F-net mechanisms (NIED) and stations observed vertical motions with  $V_{non} \geq 1.0 \text{ cm/s}$ .

Then we calculate the surface-to-borehole spectral ratios  $H/H_B$  and  $V/V_B$  of the strong motions and weak motions for horizontal and vertical components, respectively. S-wave time windows with duration of 40 s are used. Weak motions with horizontal PGAs from 20 to 100  $\text{cm/s}^2$  observed at stations where strong

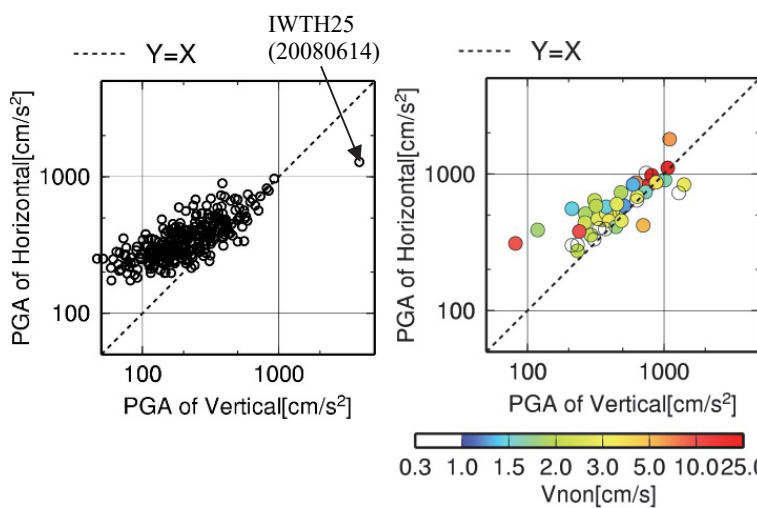


Fig. 3 – PGAs of horizontal and vertical components of 305 strong motions without Vnon (left) and with Vnon (right)

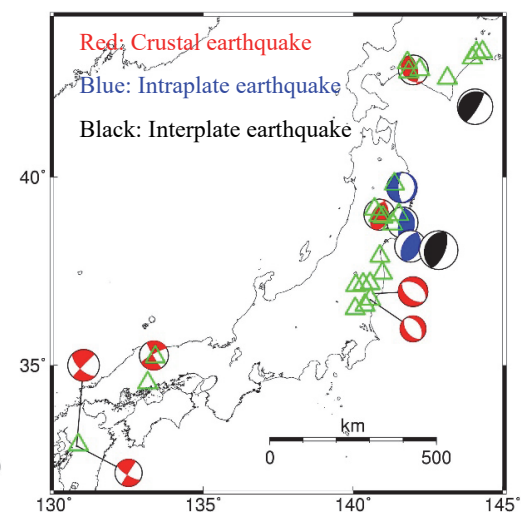
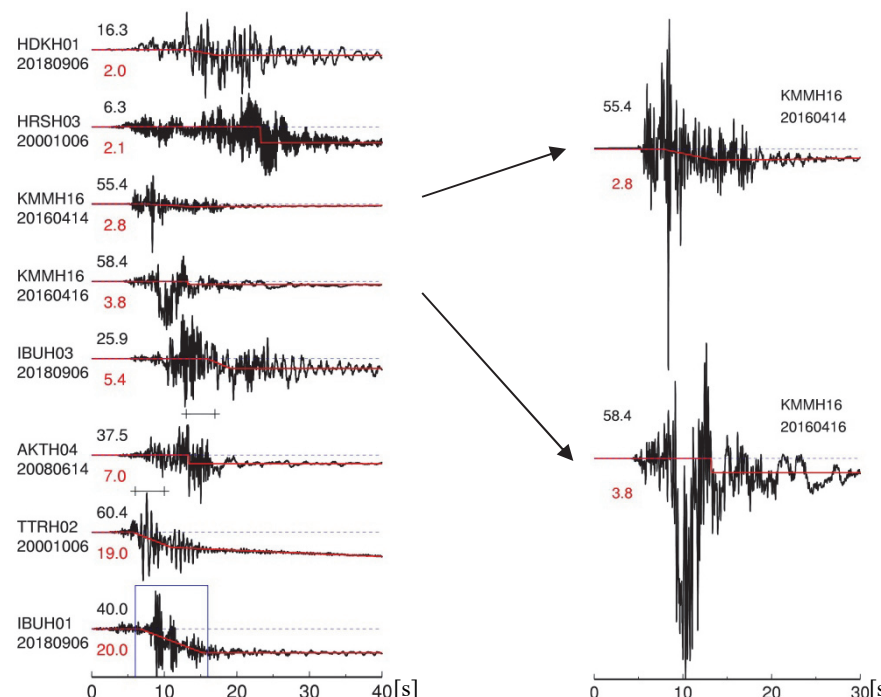


Fig. 4 – Locations of the epicenters and stations (triangles) observed vertical motions with  $V_{non} \geq 1.0 \text{ cm/s}$



(a) Eight stations with  $V_{non} \geq 2.0 \text{ cm/s}$       (b) Enlarged waveforms at KMMH16 in (a)

Fig. 5 – Velocity waveforms of vertical motions with  $V_{non} \geq 2.0 \text{ cm/s}$  for crustal earthquakes



motions with  $V_{non} \geq 1.0$  cm/s are observed are selected. By comparing the surface-to-borehole spectral ratios of weak motions with those of strong motions, the existence of nonlinear site response is identified. We will discuss the relation between the nonlinear site responses of vertical motions and  $V_{non}$ .

### 3. Velocity waveforms and site responses

Fig.5 (a) shows velocity waveforms of vertical motions with  $V_{non} \geq 2.0$  cm/s for crustal earthquakes. The number below the station name denotes the year, month and day of the earthquake origin time (JST). The waveform with the largest  $V_{non}$  is the same to Fig.1. The waveform with the second largest  $V_{non}$  is observed at KiK-net Hino (TTRH02) during the 2000 Mw6.7 Tottori-ken Seibu earthquake (20001006). This waveform is modeled by Model-i+. In Fig.5 (b) waveforms at KiK-net Mashiki (KMMH16) during the 2016 Mw7.0 Kumamoto earthquake and the Mw6.1 foreshock are enlarged. Velocity waveforms of vertical motions with large  $V_{non}$  for intraslab earthquakes and interplate earthquakes are shown in Fig.6. The vertical motion with the largest  $V_{non}$  among all KiK-net records is observed at KiK-net Haga (TCGH16) during the 2011 Mw9.0 Tohoku earthquake. Strong motions at TTRH02, KMMH16 (20160416), and TCGH16 were equivalent to JMA seismic intensity scale of 7 [4].

In Fig.7 surface-to-borehole spectral ratios of horizontal motions  $H/H_B$  and those of vertical motions  $V/V_B$

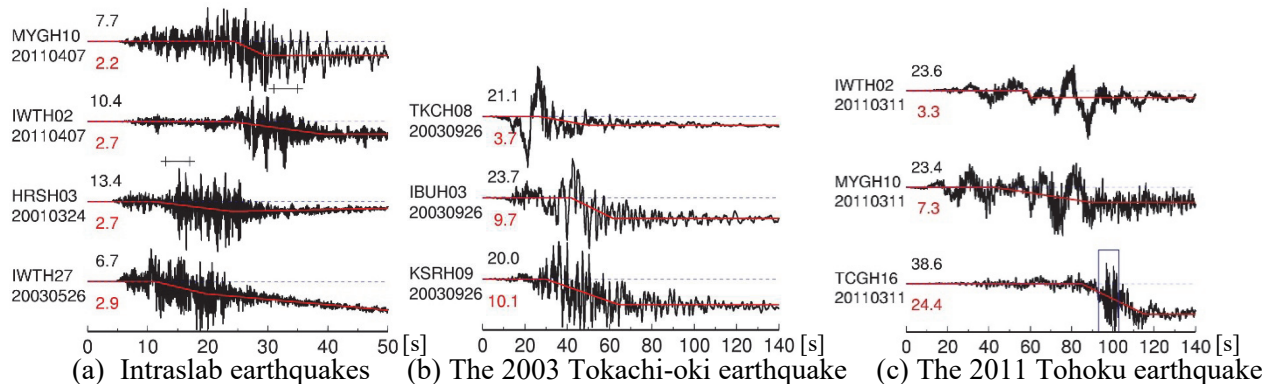


Fig. 6 – Velocity waveforms of vertical motions with large  $V_{non}$  for intraslab and interplate earthquakes

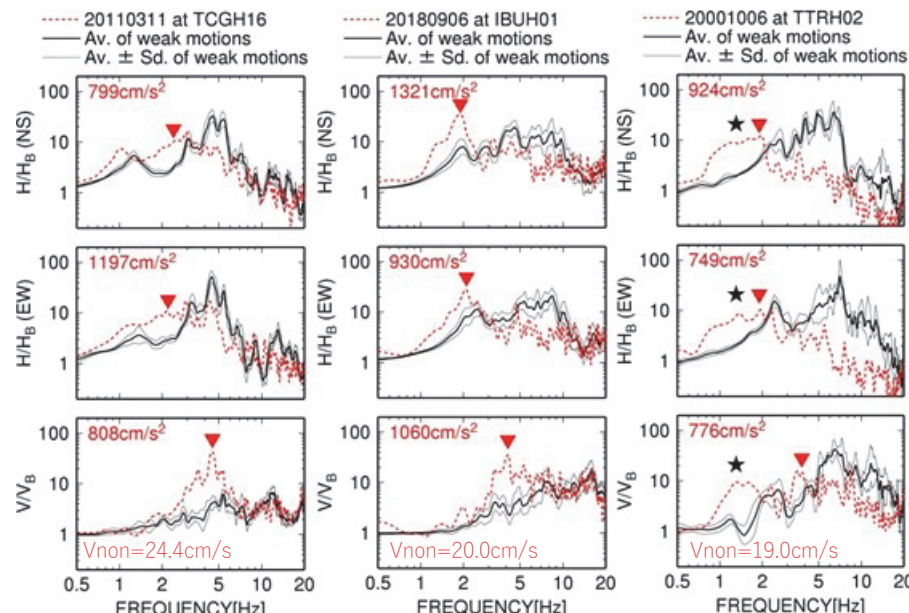


Fig. 7 – Comparison between surface-to-borehole spectral ratios for weak motions and strong motions at three stations with largest  $V_{non}$

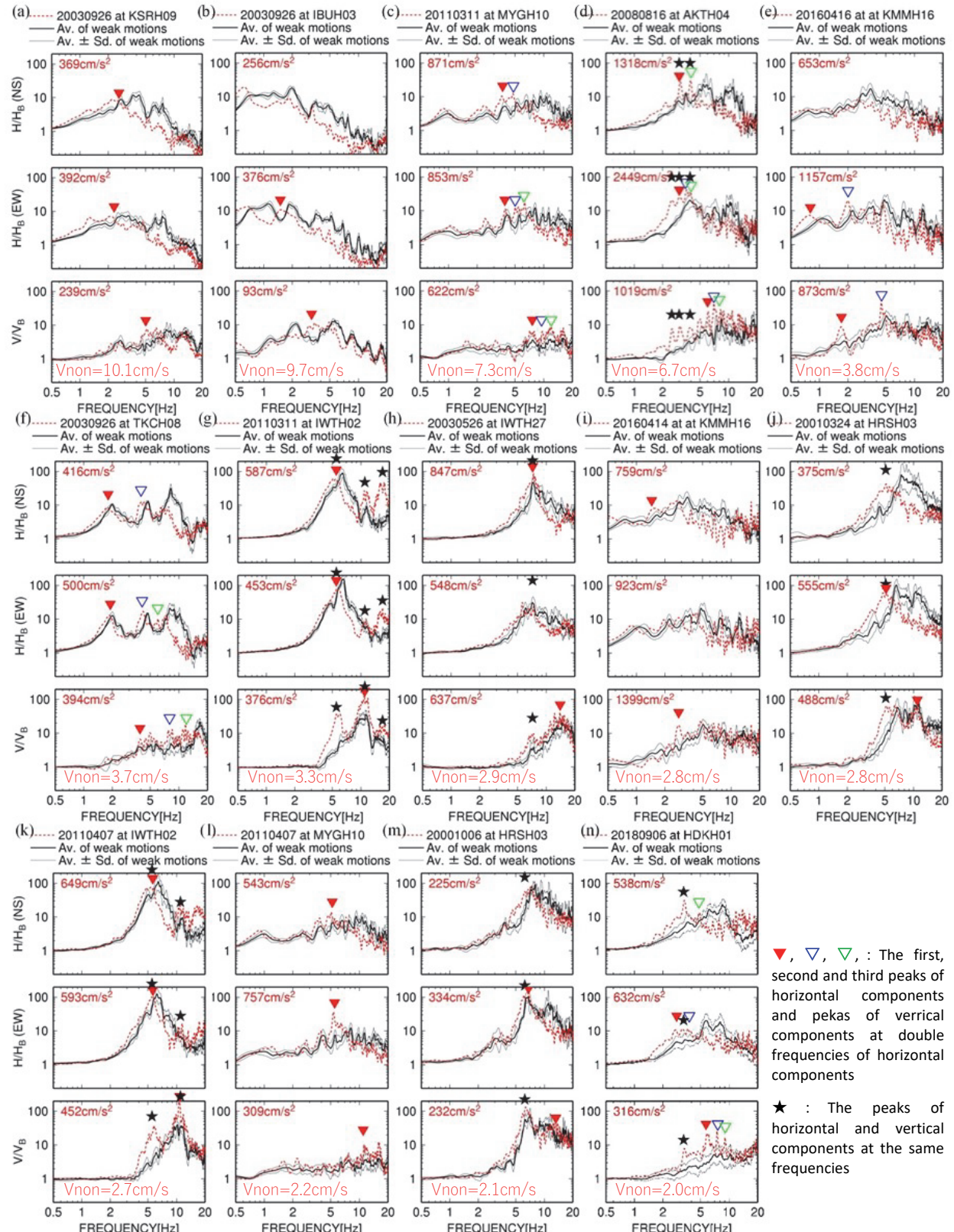


Fig. 8 – Comparison between surface-to-borehole spectral ratios for weak motions and strong motions shown in Fig.5 and Fig.6 except three station in Fig.7



for strong motions observed at three stations with the largest three  $V_{non}$  are compared with  $H/H_B$  and  $V/V_B$  for weak motions.  $H/H_B$  is calculated for the north-south (NS) component and east-west (EW) component. Both  $H/H_B$  and  $V/V_B$  for strong motions are different from those for weak motions. This result shows that vertical motions as well as horizontal motions behave nonlinear in site responses. The peak frequencies of  $V/V_B$  of strong motions are double of those of  $H/H_B$  as marked by red triangles. This is the same to the feature of the dilatancy effects [1, 2]. Satoh [7] showed that the peaks at 2 Hz of horizontal components at TCGH16 could not be reproduced by the equivalent linear analysis. Satoh [7] also showed that JMA seismic intensity scale of the synthetics without amplifications at 2 Hz did not reach 7. The peaks at 2 Hz can be interpreted to be amplified due to the dilatancy.  $V/V_B$  of the strong motion at TTRH02 also has the other peak at the same frequency to  $H/H_B$ . The peak amplitudes of  $V/V_B$  of strong motions are much larger than those of weak motions at TCGH16 and IBUH01.

In Fig.8  $H/H_B$  and  $V/V_B$  for strong motions shown in Fig.5 and Fig.6 are compared with those for weak motions. Three stations shown in Fig.7 and IBUH03 (20180906) where borehole records were contaminated by noise were not shown. Vertical motions as well as horizontal motions have nonlinear site responses. The  $V/V_B$  has the peak at double frequency or the same frequency of  $H/H_B$  in the same way to Fig.7. The  $V/V_B$  shown in Fig.8 (c), (d), (f), (g) and (n) also have the second or third peaks at double frequencies of  $H/H_B$  marked by blue or green triangles. The peak amplitudes of  $V/V_B$  for strong motions are also larger than those for weak motions in general, though the differences between  $V/V_B$  for strong motions and weak motions are smaller than those at TCGH16 and IBUH01. The peak amplitudes of  $H/H_B$  at half of peak frequencies of  $V/V_B$  tend to be larger than those of weak motions.

In order to quantify the difference between the spectral ratios for strong motions and weak motions, the ratios of  $H/H_B$  of strong motions to weak motions and the ratios of  $V/V_B$  of strong motions to weak motions are calculated. Fig.9 (a) shows the ratios averaged from 0.5 to 10 Hz and Fig.9 (b) shows the ratios averaged from 0.5 to 2 Hz. Most of the ratios of  $V/V_B$  averaged from 0.5 to 10 Hz are larger than 1.0 except those observed at stations where the lowest S wave velocity is less than 100 m/s. This result means that strong motions of vertical components are amplified compared with the weak motions by nonlinear site responses in this frequency range on the average. On the other hand, most of the ratios of  $H/H_B$  averaged from 0.5 to 10 Hz are less than 1.0. This is the typical feature of nonlinear site responses of horizontal motions. Most of the ratios of  $V/V_B$  and  $H/H_B$  averaged from 0.5 to 2 Hz are larger than 1.0. Since this frequency range is important to the damage to ordinal structures, the estimation of nonlinear site responses are important in this point of view.

Fig.10 shows the relation between  $V_{non}$  and duration of vertical motions. The duration is the time where the energy go from 5% to 95% of the total energy of acceleration records of vertical components. The

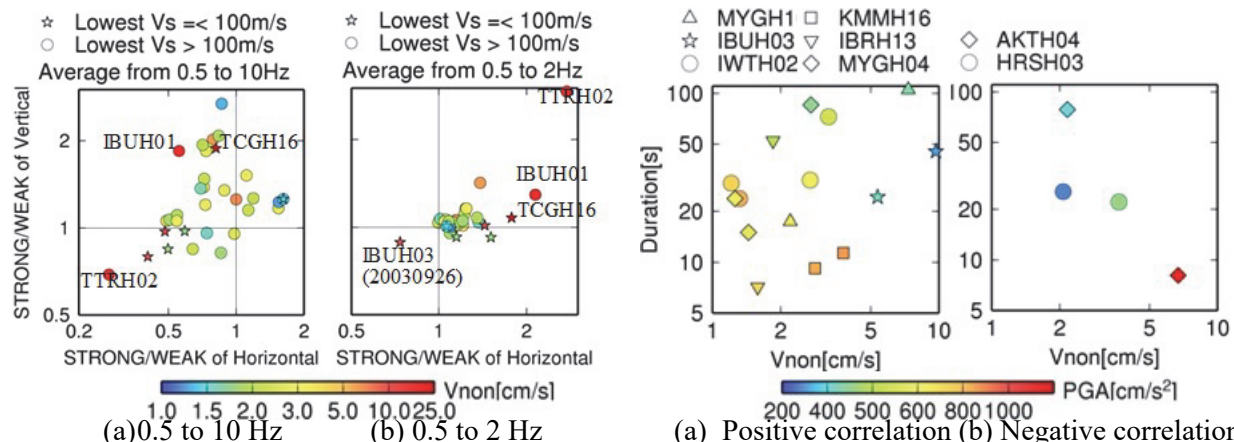


Fig. 9 – The relation between the ratios of  $H/H_B$  of strong motions to weak motions and the ratios of  $V/V_B$  of strong motions to weak motions averaged in the frequency range from 0.5 to 10 Hz and 0.5 to 2Hz

Fig.10 – The relation between  $V_{non}$  and duration of vertical motions at stations where more than two strong motions with  $V_{non} \geq 1.0$  cm/s are observed



stations where more than two strong motions with  $V_{non} \geq 1.0$  cm/s are observed are shown. The relation between  $V_{non}$  and duration is examined at the same station because nonlinear site responses strongly depend on soil properties and shallow structures. At stations shown in Fig.10 (a) a positive correlation is observed between  $V_{non}$  and the duration. This shows that  $V_{non}$  depends on duration. Although a negative correlation is observed between  $V_{non}$  and the duration at two stations shown in Fig.10 (b), this is because the PGA with shorter duration is larger than PGA of the other strong motion.

As shown in Fig.3  $V_{non}$  was not observed in strong motions observed at IWTH25 in spite of PGA of the vertical component was largest ( $3866\text{ cm/s}^2$ ) among all KiK-net records. The acceleration record and the velocity waveform of the vertical component are shown in Fig.11.  $H/H_B$  and  $V/V_B$  for strong motions at IWTH25 are compared with those for weak motions in Fig.12. The nonlinear site responses are observed in horizontal motions, but not in vertical motions. It is found that  $V_{non}$  is the good index to identify the existence of nonlinear site responses of vertical motions.

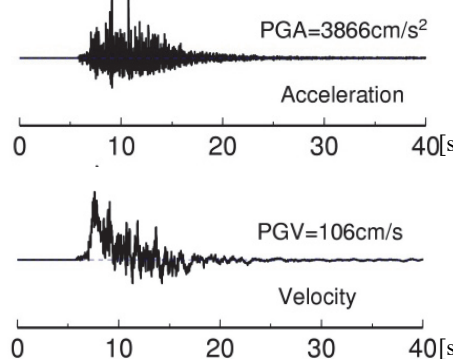


Fig. 11 – The acceleration record (above) and the integrated velocity record (below) of vertical component observed at the ground surface of KiK-net Ichinoseki-Nishi (IWTH25) during the 2008 Mw6.8 Iwate-Miyagi Nairiku earthquake (20080614).

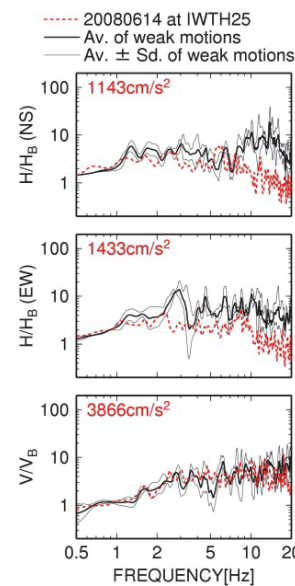


Fig. 12 – Comparison between surface-to-borehole spectral ratios for weak motions and strong motions at IWTH25

#### 4. Acceleration waveforms and the particle orbits

We discuss the causes of nonlinear site responses of vertical motions and the generation of  $V_{non}$  using acceleration waveforms and the particle orbits. Fig.13 shows the acceleration waveforms of horizontal and vertical components and their particle orbits at TCGH16 and IBUH01 in the time window shown by rectangles in Fig.6 (c) and Fig.5 (a). TCGH16 and IBUH01 are stations with the first largest and the second largest  $V_{non}$ , respectively. X-axis and Y-axis of the orbits are horizontal and vertical directions, respectively. The shape of orbits is upward convex, downward convex or butterfly shaped suggesting rotational motions. The tips of peaks of acceleration waveforms of horizontal motions in Fig.13 are splitting. The absolute accelerations of the time windows of vertical components shown by bars in Fig.13 are shown in Fig.14. The acceleration waveforms of vertical motions have sharp large peaks in the upward (positive) direction shown by blue lines and have relatively small peaks in the downward (negative) direction shown by green lines.

Morio et al. [2] showed these features of waveforms of both vertical and horizontal components by elasto-plastic dynamic response analysis for dry sands. Morio et al. [2] pointed out that the upward and downward convex particle orbits are generated due to negative and positive dilatancy, respectively. Hinokio et al. [8] pointed out that unsaturated sands ended up contraction in volume, that is, the negative dilatancy while showing both positive and negative dilatancy during the cyclic loading and then became steady states.



Iwamoto et al. [9] also showed the negative dilatancy for unsaturated gravelly sands by cyclic loading tests. Therefore the particle orbits of accelerations shown in Fig.13 suggest the generation of the dilatancy. The velocity waveforms with Vnon would be caused by the negative dilatancy.

Fig.15 shows acceleration waveforms of horizontal and vertical components at four stations. TTRH02

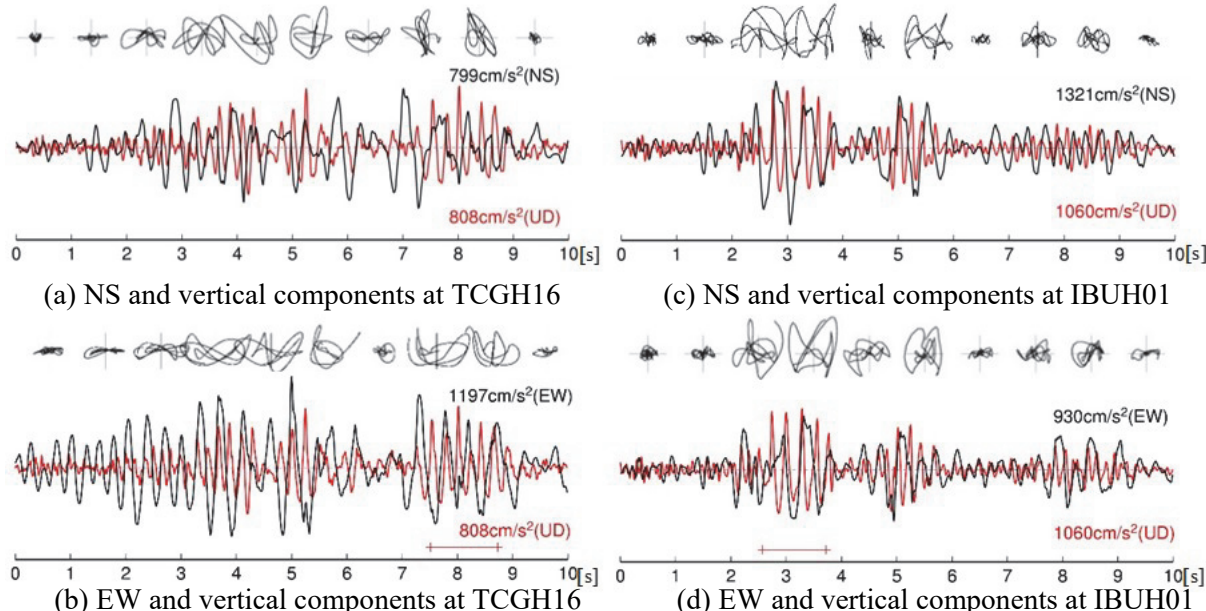


Fig. 13 – Acceleration records of horizontal (black) and vertical (red) components in the time windows shown by rectangles in Fig.6 (c) and Fig.5 (a) and the particle orbits at TCGH16 and IBUH01

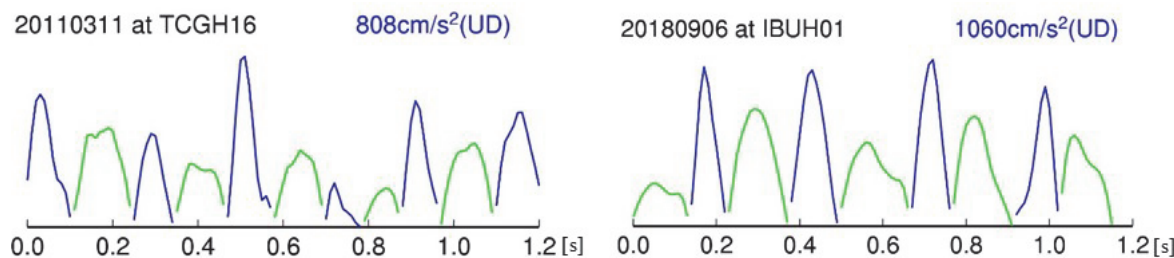


Fig. 14 – The absolute accelerations of the time windows of vertical components shown by bars in Fig.13. Blue and green lines are the positive and negative amplitudes in Fig. 13, respectively.

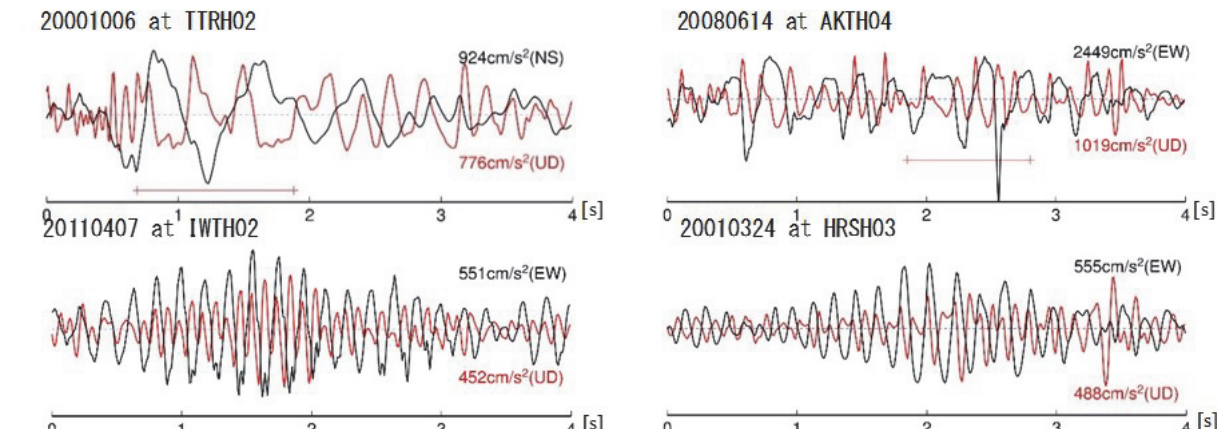


Fig. 15 – Acceleration records of horizontal (black) and vertical (red) components in the time windows shown in Fig.5 (a) and Fig.6 (a) by bars at TTRH02, AKTH04, IWTH02 and HRSH03



and AKTH04 are the stations with the third and the seventh largest Vnon, respectively. At IWTH02 (Tamayama) and HRS03 (Mishirabe) the peak frequencies of vertical components are the same to those of horizontal components as shown in Fig.8 (k) and (j). The acceleration waveforms of vertical motions at TTRH02 and AKTH04 in the time window shown by bars shave sharp large peaks in the upward (positive) direction and have relatively small peaks in the downward (negative) direction. This is the same feature to acceleration waveforms at TCGH16 and IBUH01. On the other hand, acceleration waveforms at IWTH02 and HRS03 do not have such features. The causes why vertical motions are predominant at the same frequencies to horizontal components are not unknown but might be the tilt of the ground.

## 5. Application to K-NET and JMA strong motion records

In order to confirm that Vnon is observed in strong motions recorded by the different seismometers from KiK-net, we calculate velocity time histories from acceleration records observed at K-NET and JMA strong motion stations.

Fig.16 shows the acceleration and vertical waveforms observed at K-NET Tsukidate (MYG004) during the 2011 Mw9.0 Tohoku earthquake. The PGAs of horizontal and vertical components were large as shown by black numbers in  $\text{cm/s}^2$ . The velocity waveform of the vertical component has two steps after S-wave portions from two strong motion generation areas of SMGA1 and SMGA2 [10]. The total Vnon is 34  $\text{cm/s}$ , which is larger than Vnon at TCGH16 with the largest Vnon among all KiK-net records. Acceleration records in the time window shown in Fig.16 by blue rectangles and the particle orbits of NS and UD components are shown in Fig.17. The upward convex shape is clearly observed in particle orbits as pointed out by previous studies [2, 11]. The particle orbits suggest the rotational motions. Fig.18 shows acceleration

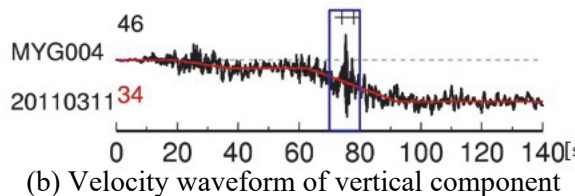
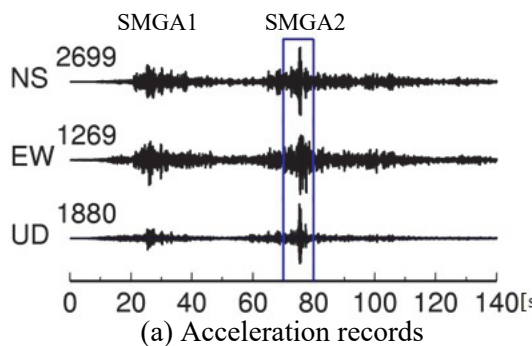


Fig. 16 – Acceleration and velocity waveforms observed at K-NET Tsukidate (MYG004) during the 2011 Mw9.0 Tohoku earthquake

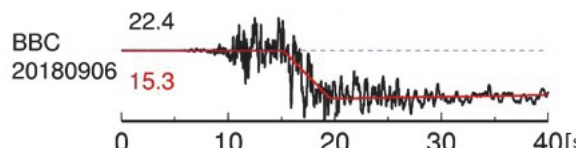


Fig. 19 – Velocity waveforms of vertical components observed at JMA Atsuma Shikanuma (BBC) and K-NET Oiwake (HKD127) during the 2018 Mw6.6 Hokkaido Iburi-Tobu earthquake

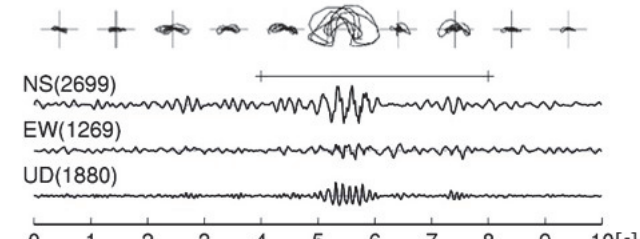


Fig. 17 – Acceleration records in the time window shown in Fig.16 by blue rectangles and the particle orbits of NS and UD components at MYG004

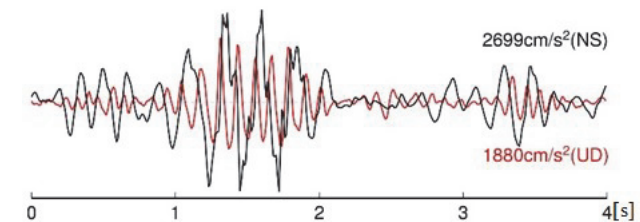
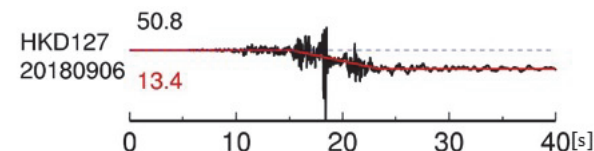


Fig. 18 – Acceleration records of horizontal (black) and vertical (red) components in the time windows shown in Fig.16 and Fig.17 by bars at MYG004





records of horizontal and vertical components in the time windows shown in Fig.16 and Fig.17 by bars. Both horizontal and vertical waveforms have the same features to those at TCGH16 and IBUH01. Motosaka [11] showed that vertical components are predominant at double frequencies of horizontal components. As mentioned in “Introduction”, Morio et al. [2] showed by analytical studies that the strong motions at MYG004 were affected by the dilatancy.

Fig.19 shows velocity waveforms of vertical components observed at JMA Atsuma Shikanuma (BBC) and K-NET Oiwake (HKD127) during the 2018 Mw6.6 Hokkaido Iburi-Tobu earthquake. JMA seismic intensity scale of 7 were observed at both stations. BBC is located at 5 km away from KiK-net Atsuma (IBUH03) that velocity waveform is shown in Fig.5 (a). HKD127 is located at 0.1 km away from IBUH01 that velocity waveform is shown in Fig.1 and Fig.5 (a). Vnon at BBC and HKD127 was the fourth and fifth largest if these data are included in KiK-net records. Since the dilatancy influenced on both horizontal and vertical site responses, these large ground motions might be affected by the nonlinear site responses including the negative dilatancy of unsaturated soil. The spiky acceleration records at IBUH01 or TCGH16 shown in Fig. 13 might be caused by cyclic mobility and the increase of excess pore water pressure might occur. In this case, Vnon would be generated by the settlement due to the dissipation of excess pore water pressure.

## 6. Conclusions

In this study we show that the existence of nonlinear site responses of vertical motions is identified by velocity waveforms integrated from acceleration records observed at the ground surface. In the case of the generation of nonlinear site responses of vertical motions, the velocity waveform has a linear trend to the downward direction and then becomes constant or almost constant. In some cases, the velocity time history abruptly becomes constant like the step function. We define the absolute constant value as Vnon. The surface-to-borehole spectral ratios of vertical strong motions with Vnon have the peaks at the same or double of the peak frequencies of the horizontal strong motions. The features that the predominant frequencies of vertical motions are double of those of horizontal motions suggest dilatancy effects as pointed out by experimental or analytical studies on elasto-plastic dynamic of soil (e.g. [1, 2]). The spectral ratios of vertical strong motions tend to be larger than those of weak motions in the frequency less than about 10 Hz. The peak amplitudes of spectral ratios of horizontal strong motions at half of peak frequencies of vertical strong motions also tend to be larger than those of weak motions. The strong motions with three largest Vnon were records observed at KiK-net Haga during the 2011 Tohoku earthquake, KiK-net Oiwake during the 2018 Hokkaido Iburi-Tobu earthquake and KiK-net Hino during the 2000 Tottori-ken Seibu earthquake. These strong motions were equivalent to JMA instrumental seismic intensity scale of 7. The acceleration waveforms and the particle orbits show the features suggesting the dilatancy shown by Morio et al. [2]. The Vnon of K-NET Tsukidate with JMA instrumental seismic intensity scale of 7 was the largest among all KiK-net records. Since the dilatancy influenced on both horizontal and vertical site responses, these large ground motions might be affected by nonlinear site responses with the dilatancy. The other plausible interpretation of Vnon is the settlement of the ground due to the dissipation of the excess pore water pressure, since some acceleration records have spiky-shape suggesting the increase of the excess pore water pressure.

## Acknowledgements

We use KiK-net records, K-net records and F-net mechanisms by NIED (National Research Institute for Earth Science and Disaster Resilience). We also use the hypocenter information and strong motion records by JMA (Japan Meteorological Agency). GMT [12] is used for plotting figures.



## References

- [1] Ohshima Y, Watanabe H (1994): An experimental study on elasto-plastic dynamic interaction of 3-D underground structure and soil. *Earthquake Engineering & Structural Dynamics, Journal of JSCE*, **489** (I-27), 261-268. (in Japanese)
- [2] Morio S, Kato Y, Fujii T (2017): Elasto-plasticity consideration of the ground on the large acceleration time histories at two earthquake observation sites, *Journal of JAEE*, **17**(4), 30-49. (in Japanese)
- [3] Satoh T (2020): Study on identification of nonlinear site responses of vertical motions using strong motion records observed at the ground surface, *Journal of JAEE*, accepted. (in Japanese)
- [4] National Research Institute for Earth Science and Disaster Resilience (2019): NIED K-NET, KiK-net, National Research Institute for Earth Science and Disaster Resilience, doi:10.17598/NIED.0004.
- [5] Javelaud EH, Ohmachi T, Inoue S (2011): A quantitative approach for estimating coseismic displacements in the near field from strong-motion accelerographs, *Bull. Seism. Soc. Am.*, **101** (3), 1182–1198.
- [6] Satoh T (2018): Study on long-period pulse and permanent displacement of the 2016 Kumamoto earthquake based on comparison with previous prediction equations, *J. Struct. Constr. Eng., AJJ*, **750**, 1117-1127. (in Japanese)
- [7] Satoh T (2016): Causes of large ground motions at K-NET Tsukidate and KiK-net Haga during the Tohoku earthquake based on the analysis of weak and strong motion records, *Journal of JAEE*, **16** (4), 52-65. (in Japanese)
- [8] Hinokio M, Nakai T, Hoshikawa T, Yoshida H (2001): Stress strain behavior of sand under monotonic and cyclic loading in general stress system and its elastoplastic modeling, *Soils and Foundations*, **4** (3), 107-124 (in Japanese)
- [9] Iwamoto I, Kokusho T, Nakano T (2003): Volume change characteristics of gravelly sands by means of monotonic and cyclic shear test, *Journal of JSCE*, **17** (III-63), 205-215. (in Japanese)
- [10] Satoh T (2012): Inversion of source model of the 2011 off the pacific coast of Tohoku earthquake using empirical Green's function method, *15<sup>th</sup> World Conference on Earthquake Engineering*, Lisbon, Portugal, WCEE2012\_0974.pdf.
- [11] Motosaka M (2012): Lessons of the 2011 Great East Japan earthquake focused on characteristics of ground motions and building damage, *International symposium on engineering lessons learned from the 2011 great east Japan earthquake*, Tokyo, Japan, 166-185.
- [12] Wessel P, Smith WHF (1998): New, improved version of Generic Mapping Tools released, *EOS, AGU*.